GEOPHYSICAL RESEARCH LETTERS, VOL. 36, L15707, doi:10.1029/2009GL039050, 2009

Parametric uncertainty effects on aerosol radiative forcing

J. O. Haerter,[1] E. Roeckner,[1] L. Tomassini,[1] and J.-S. von Storch[1]

Received 11 May 2009; revised 9 July 2009; accepted 16 July 2009; published 13 August 2009.

[1] Among the known radiative forcings, the fourth IPCC assessment report estimates the aerosol radiative forcing to harbor the widest range of uncertainty extending from -1.8 to -0.3 W/m^2. The IPCC estimates focus mainly on structural uncertainties, including uncertainties in aerosol sources. Here, we study the uncertainty of the sulfate aerosol radiative forcing due to parametric uncertainty in a state-of-the-art general circulation model (GCM). Numerical experiments were carried out by perturbing seven cloud parameters in the model. We find that the uncertainty due to a single one of these parameters can be as large as 0.5 W/m^2, and the uncertainty due to combinations of these parameters can reach more than 1 W/m^2. These numbers should be compared with the sulfate aerosol forcing of -1.9 W/m^2 for the year 2000, obtained using the default values of the parameters. The uncertainty results from a high sensitivity of cloud optical properties to aerosol concentrations, which can be amplified by changing cloud parameter setting. **Citation:** Haerter, J. O., E. Roeckner, L. Tomassini, and J.-S. von Storch (2009), Parametric uncertainty effects on aerosol radiative forcing, *Geophys. Res. Lett.*, *36*, L15707, doi:10.1029/2009GL039050.

1. Introduction

[2] Parametric uncertainty (PU) in climate models has recently drawn broad attention. In the experiments carried out with the GCM HadAM3 [*Murphy et al.*, 2004] six cloud parameters were perturbed by allowing different combinations of parameter values. In a different study by *Piani et al.* [2005], the public's computing resources were used to perform a large number of perturbed physics experiments. Both activities aimed at a better understanding of the uncertainties in climate model projections due to uncertainties in model parameters. The model was treated as a black box that serves to produce probability density functions of model output given a set of input parameters.

[3] Generally, the process that transfers PUs to uncertainties in the model output is highly complex. One possible way to study this process is to first quantify the effect of PU on radiative forcing. Important factors that determine radiative forcing are solar irradiance, volcanic eruptions, greenhouse-gas (GHG) concentrations, and aerosols. Even though these factors per se may be independent of model formulations, the processes that turn them into climate-active radiative forcing do depend on model formulations.

[4] Aerosols affect climate via the direct and indirect radiative effects [*Forster et al.*, 2007]. The direct effect is the mechanism by which aerosols scatter and absorb radiation. The indirect effect concerns changes to cloudy skies due to aerosol perturbations. While the former depends on the model radiation scheme, the latter also depends crucially on cloud parameterizations which themselves are leading sources of PU. Thus, the radiative forcing resulting from the aerosol indirect effect is intimately linked to PU.

[5] The uncertainty in aerosol forcing is a well known problem. Studies devoted to it have been summarized by *Forster et al.* [2007]. Previous work has mainly focused on *structural* uncertainties, such as uncertainties in aerosol sources, representation of aerosols in models, parameterizations that relate aerosols and cloud droplets to simulate the indirect aerosol effect, and in cloud schemes [*Textor et al.*, 2006; *Boucher and Lohmann*, 1995; *Penner et al.*, 2006; *Chen and Penner*, 2005; *Menon et al.*, 2002; *Lohmann*, 2008; *Lohmann et al.*, 2000; *McComiskey and Feingold*, 2008; *Myhre et al.*, 2004; *Roeckner et al.*, 1999]. Efforts were also made to constrain the aerosol forcing and the climate sensitivity by reconstructing the 20th century global mean temperature development within simplified climate models [*Harvey and Kaufmann*, 2002; *Kiehl*, 2007]. What has not been systematically studied are *parametric* uncertainties: Given an atmospheric GCM with a state-of-the-art representation of the aerosol direct and indirect effects, we ask for the uncertainty in aerosol forcing resulting from uncertainties in model parameters. In reconstructions of the 20th century global temperature change using numerical models, the apparent GHG and aerosol forcings were found to be statistically coupled [*Andreae et al.*, 2005]. In this context it is important to understand the impact of parameters on the resulting forcing, as this would require subsequent changes in the model GHG forcing.

[6] To study PU, we use the ECHAM5 atmospheric GCM [*Roeckner et al.*, 2003] in a horizontal resolution of T31 (corresponding to about 3.75 degree grid spacing) with 19 vertical levels. The model includes parameterizations of the direct and the first indirect aerosol effects [*Boucher and Lohmann*, 1995]. The latter is based on an empirical relation between aerosol concentration and cloud droplet number concentration. Increased number concentration diminishes the effective cloud droplet radius that in turn controls the optical properties of clouds. Smaller cloud droplets produce larger albedo. A higher-resolution version of this model has been used for the IPCC AR4 climate change experiments (details in auxiliary material).[2]

2. Methods and Experiments

2.1. Definition of the Aerosol Radiative Forcing

[7] To isolate the sulfate aerosol radiative forcing (in the following *aerosol forcing*), the ECHAM5 model is

[1]Max Planck Institute for Meteorology, Hamburg, Germany.

0094-8276/09/2009GL039050$05.00

[2]Auxiliary materials are available in the HTML. doi:10.1029/2009GL039050.

Table 1. List of Parameters, Description, Minimum, Maximum and Default Values

Parameter	Description and Reference	Minimum	Maximum	Standard
ε_{sc}	entrainment rate for shallow convection [*Tiedtke*, 1989]	10^{-4}	10^{-3}	3×10^{-4}
ε_{pc}	entrainment rate for penetrative convection [*Tiedtke*, 1989]	0	2×10^{-4}	1×10^{-4}
β	cloud mass flux above non-buoyancy level [*Tiedtke*, 1989]	0.1	0.5	0.3
a_{corr}	correction to asymmetry parameter for ice clouds [*Stephens et al.*, 1990]	0.8	1.0	0.91
χ_l	inhomogeneity parameter for liquid clouds [*Cahalan et al.*, 1994]	0.5	1.0	0.7
χ_i	inhomogeneity parameter for ice clouds; analogous to χ_l but for ice	0.5	1.0	0.7
G_p	conversion efficiency from cloud water to precipitation [*Tiedtke*, 1989]	2×10^{-4}	10^{-3}	4×10^{-4}

subjected to two prescribed sulfate aerosol (*aerosol*) distributions. The first, referred to as C_0, represents a background aerosol loading that is needed to produce cloud droplets in the control run [*Tanré et al.*, 1984]. The second (denoted $C_0 + C_1$) uses the background aerosol loading C_0 plus the natural and anthropogenic aerosol burden of the year 2000 [*Haywood and Boucher*, 2000]. Pairs of integrations were carried out, in which the ECHAM5 model was forced by the C_0- and $C_0 + C_1$-aerosol distribution, respectively. As the model atmosphere responds quickly to the change in aerosol loading it reaches a statistical equilibrium state within a few weeks. The model was integrated for 10 years to reduce the impact of natural variability. The aerosol forcing F is defined as the change in the top of the atmosphere (TOA) radiative forcing

$$F \equiv \left(\bar{P}_{sw}^{C_0+C_1} + \bar{P}_{lw}^{C_0+C_1}\right) - \left(\bar{P}_{sw}^{C_0} + \bar{P}_{lw}^{C_0}\right) \quad (1)$$

where the overbar indicates the 10-year global mean, $\bar{P}_{sw}^{C_0+C_1}$ and $\bar{P}_{lw}^{C_0+C_1}$ ($\bar{P}_{sw}^{C_0}$ and $\bar{P}_{lw}^{C_0}$) are the net (upward plus downward) TOA short and long wave radiation obtained by forcing the model with the $C_0 + C_1$ (C_0) aerosol distribution. F includes both the direct and the first indirect effect. To isolate the latter, we consider also F_{clsky} which results from F by replacing $\bar{P}_{sw}^{C_0}$ by $\bar{P}_{sw,clsky}^{C_0}$ and similarly for the other terms in equation (1) and the fluxes at the TOA are then taken only under clear-sky conditions.

[8] Note that equation (1) defines the total aerosol radiative forcing resulting from both the natural and the anthropogenic aerosol changes and that F defined in equation (1) includes responses of the atmosphere to the given aerosol loading. This is done deliberately, since the aerosol forcing, in particular the indirect effect, can only fully evolve by allowing the atmospheric state to adjust to the aerosol loading [*Hansen et al.*, 2005; *Knutti and Hegerl*, 2008]. We exclude the slow ocean feedback.

2.2. Parameters to be Perturbed

[9] While other parameters may likely contribute to the uncertainty, we focus on seven cloud model parameters (Table 1) that are particularly uncertain (details in auxiliary material), but relevant for cloud optical properties. While aerosol effects are allowed to modify large-scale clouds in the model, large-scale and convective clouds interact, e.g., through modifications to the ambient humidity. The entrainment parameters ε_{sc}, ε_{pc} and the mass-flux parameter β can affect cloud water content and size. Large values of ε_{sc} (ε_{pc}) can lead to an increase in cloud water content and larger cover of low level (high penetrating) clouds. Smaller values of β repress evaporation of clouds and sustain clouds, and vice versa for large values of β. The asymmetry correction factor a_{corr} as well as the inhomogeneity parameters χ_i and χ_l control the microphysical properties of clouds. G_p determines the conversion efficiency of convective cloud water to precipitation. Similar parameterization schemes are likely to be implemented in other GCMs as well. The seven parameters are perturbed within the ranges given in Table 1. The ranges are chosen by expert elicitation and allow realistic climate simulations. To assess the realism of the configurations we have compared the TOA radiation balance with the default setting and analyzed a set of skill-scores. We have assessed initial condition uncertainty by employing different starting conditions for the same set of parameters (details in auxiliary material).

2.3. Single-parameter Perturbation (SPP) Experiments

[10] In the first set of experiments, we systematically modify only one parameter at a time while keeping all others fixed to their standard values (Table 1). Ten values equally spaced between the lower and upper bounds given in the table are sampled for all parameters but ε_{sc}, where nine values are considered. For each set of parameters, two integrations were carried out, one driven by C_0, the other by $C_0 + C_1$. In total, 69 pairs of integrations were performed and analyzed.

[11] Figure 1 shows that the all-sky aerosol forcing F is always negative. F obtained from the standard parameter values is -1.9 W/m^2. This value results mainly from the indirect effect related to clouds. The direct effect, which can be quantified by the TOA radiation change under clear sky conditions, accounts for only -0.5 W/m^2 (not shown).

[12] Figure 1 also shows the parameter-dependence of F. It depends strongly on ε_{sc} and β (Figure 1a). The negative forcing is enhanced with increasing values of ε_{sc} and decreasing values of β. The range of uncertainty in F due to ε_{sc} and β is about 0.35 W/m^2 and 0.65 W/m^2, respectively. Both uncertainty ranges are much larger than the uncertainty induced by the internal variability (gray bars). F shows also some dependence on a_{corr} and χ_l (Figure 1b). However, the dependence is much less stable in the sense that the value of F changes abruptly with increasing values of a_{corr} and χ_l. F depends little on χ_i, ε_{pc} and G_p (Figure 1c).

[13] ε_{sc} and β affect F mainly through liquid cloud water. An increase in ε_{sc} leads to an increase in clouds, in particular in cloud water content (details in auxiliary material). Under clear-sky conditions, the aerosol forcing becomes insensitive to cloud parameter changes (not shown).

[14] While the short-wave component roughly follows the development of the total aerosol forcing, the long-wave component is insensitive to parameter changes in all seven cases (Figure 1). Furthermore, the long-wave contribution is always positive and on the order of +0.2 W/m^2. This is a

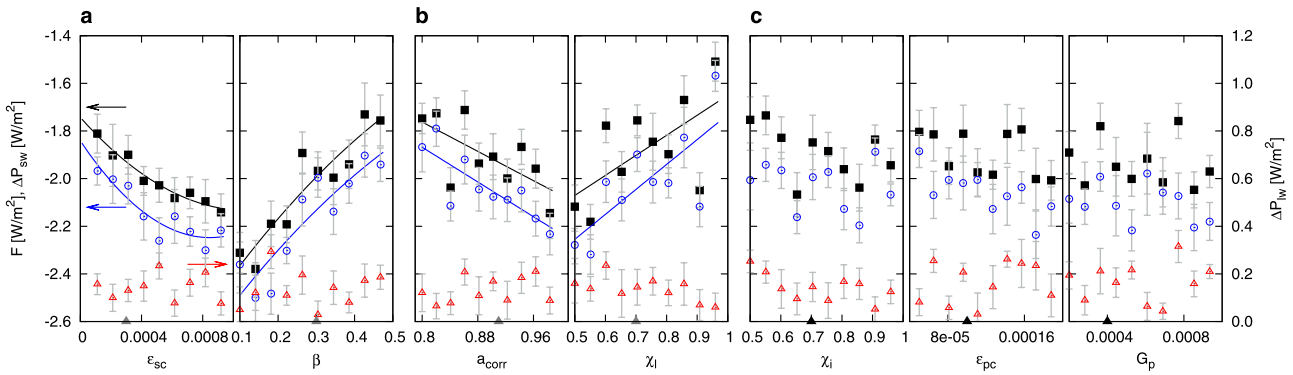

Figure 1. Dependence of F on (a) ε_{sc} and β on (b) a_{corr}, χ_l and on (c) χ_i, ε_{pc} and G_p obtained from SPP experiments. Symbols are 10-year mean values obtained from each experiment for total aerosol forcing (black solid squares), its short wave component (blue circles) and its long-wave component (red triangles, right vertical axis). Lines represent polynomial fits to respective values for total forcing (black curves) and short-wave component (blue curves). Gray error bars correspond to standard deviations of 10-year means. Gray triangles are default parameter values.

negative feedback that is understood within a black-body picture of the Earth-system.

2.4. Multi-parameter Perturbation (MPP) Experiments

[15] In a second set of experiments we allow all parameters to vary simultaneously using a Latin hypercube (LH) sample [*McKay et al.*, 1979] with $N = 100$ distinct parameter sets, enabling us to identify non-linear interactions between parameters. This random sampling ensures that all N values of each parameter are used once. For each parameter set, we then carry out pairs of experiments driven by the C_0- and $C_0 + C_1$-distribution. A total of 100 pairs of 10-year experiments were carried out.

[16] Figure 2a shows F obtained from the 100 LH-experiments. To describe changes in F due to parameter-combinations, we sort the simulated values according to the sum $g(\mathbf{x}) \equiv \sum_i c_i(x_i - x_{0,i})/(x_i^{\max} - x_i^{\min})$ for $\mathbf{x} = \{\varepsilon_{sc}, \beta, g, \chi_l\}$. The factors $c_i = \{-1, 1, -1, 1\}$ are chosen to allow the emergence of maximal possible values of F. $\mathbf{x}_0$ is the default parameter vector and i specifies the i'th component. F varies now from -3 W/m^2 to -1.6 W/m^2 and clearly depends on $g(x)$. This dependence means that the effects of the individual parameter perturbations manifest in a joint manner in MPP. As may be expected, the effect of the parameter combination is much larger than that found for any of the individual variations shown in Figure 1.

[17] What remains still unclear is whether this large uncertainty range is caused by non-linear interactions between changes due to the four parameters, or represents a linear superposition of the isolated effects of the parameters. To address this issue, we rewrite $F(\mathbf{x}_0 + \delta\mathbf{x})$ obtained from a set of perturbed parameters $\mathbf{x}_0 + \delta\mathbf{x}$ as $F(\mathbf{x}_0 + \delta\mathbf{x}) = F(\mathbf{x}_0) + \sum_i F_i(\mathbf{e}_i \cdot \delta\mathbf{x}) + F^{int}(\delta\mathbf{x})$, where $\mathbf{e}_i$ is the unit vector in the direction of the i'th perturbed parameter, $F_i(\mathbf{e}_i \cdot \delta\mathbf{x})$ describe the deviations from $F(\mathbf{x}_0)$ due to SPP $(\mathbf{e}_i \cdot \delta\mathbf{x})$ and $F^{int}(\delta\mathbf{x})$ captures the interactions between the parameters.

[18] The contributions from each single parameter perturbation can be computed by reconstructing $F(\mathbf{x}_0 + \delta\mathbf{x})$ using the first two terms on the right hand side of the above equation. We derive the terms $F_i(\mathbf{e}_i \cdot \delta\mathbf{x})$ from the parameter dependence found in SPP-experiments (curves in Figure 1). The reconstructed aerosol forcing is compared with that obtained from the LH-experiments in Figures 2a and 2b.

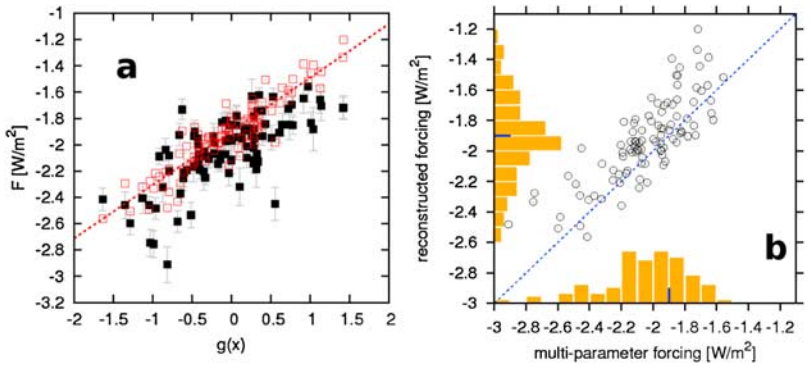

Figure 2. (a) F in MPP experiment; symbols are 10-year mean values obtained from each experiment for total aerosol forcing (black solid squares) and linear reconstructions (red open squares); dashed red line is best linear fit to reconstructed data, gray error bars correspond to standard deviations of 10-year means. (b) Scatter plot of F obtained from the MPP experiments and linear reconstructions (circles); blue solid lines indicate default forcing for reference; dashed line is slope expected if forcing results from linear superposition of the effects of individual parameters; bar chart on horizontal (vertical) axis is histogram of MPP (reconstructed) forcing.

The larger the difference between the two, the larger is the non-linear effect.

[19] In the vicinity of $F(\mathbf{x}_0)$ the points in Figure 2b scatter around the diagonal. However, there is also an overall bias for large and small values of F. That is, as F becomes larger or smaller than the value $F(\mathbf{x}_0) = -1.9$ W/m^2, the reconstructed values are larger than the values obtained from the MPP-experiments. The effect of non-linearity becomes apparent also in the histograms of the computed forcing obtained from the MPP-experiment and the reconstructions (Figure 2b). The former displays a larger probability weight for forcings smaller than the default value $F(\mathbf{x}_0)$ and the span of values with $F(\mathbf{x}) < F(\mathbf{x}_0)$ is more than twice that of the values with $F(\mathbf{x}) > F(\mathbf{x}_0)$. On the contrary, the latter shows roughly equal weight and span of values on either side of $F(\mathbf{x}_0)$.

[20] The bias obtained for large values of F is induced by an inherent upper bound of the aerosol effect. Since the aerosol indirect effect works only in the presence of clouds, F is limited by its clear-sky value of -0.5 W/m^2. One cannot further reduce the aerosol forcing, once all clouds have been removed. Consider an extreme situation in which the value of a parameter leads to a strong reduction in clouds so that the aerosol forcing is close to the clear-sky value of -0.5 W/m^2. Suppose that we have, say, two such parameters. If we perturb the atmosphere with each of these parameters separately and derive the net effect of the two parameters by linear combination, we would obtain a forcing of about -1.9 W/m^2 + 2 $\times$ (-0.5 + 1.9)W/m^2 = +0.9 W/m^2, which is now positive. On the other hand, if we perturb the atmosphere with the two parameters jointly, and if the joint effect of the two parameters is still a strong reduction in clouds, we would obtain a forcing close to the clear-sky value of -0.5 W/m^2. In this extreme example, the linear reconstruction produces a value that is much larger than that obtained from the MPP-experiment. For less extreme parameter values, similar but smaller biases of the reconstruction will be obtained. This is why the reconstructed forcing becomes increasingly larger than the true forcing, as F increases in Figure 2b. The MPP-forcing tends to be more negative than that obtained from the superpositions of individual contributions. This is particularly true for the parameter combination considered in Figure 2a, in which the difference between the reconstruction and the true value is as large as 0.4 W/m^2.

[21] Due to the inherent upper limit of the aerosol forcing but a lack of a strict lower bound, a widening of the uncertainty range of cloud parameters will tend to increase the lower end of the uncertainty range toward larger negative values while hardly changing the upper limit. Similarly, if a larger number of uncertain cloud parameters were considered, the lower bound of the uncertainty range would be extended to more negative values. In general, it is dangerous to draw conclusions about joint effects of several parameters from SPP-experiments only. Due to non-linear effects, the reconstruction can notably deviate from the true joint effect.

3. Concluding Remarks

[22] We have investigated the uncertainty in the sulfate aerosol forcing F due to the uncertainty in seven crucial cloud parameters. The paper demonstrates the high sensitivity of F to cloud parameters in the state-of-the-art atmospheric GCM ECHAM5 within perturbed physics experiments. For standard parameter-values, F amounts to -1.9 W/m^2. Two sets of experiments were carried out. In the first we varied only one parameter, keeping all others to their standard values. We found that F is sensitive to parameters which affect liquid water clouds. When varying these parameters to increase the cloud water content, F increases. The resulting uncertainty in F can be as large as 0.5 W/m^2. In the second set the seven parameters were varied according to a random sampling. Combinations of parameters led to an uncertainty in F of about 1.5 W/m^2. Even though changes due to individual perturbations can be linearly superimposed in the vicinity of the default setting $\mathbf{x}_0$, substantial non-linear modifications do occur further away from $\mathbf{x}_0$.

[23] So far future projections have been - for a given climate model - derived using a 'standard' set of cloud parameters that produce realistic present-day climate. There may exist another set of parameters that produces a similar present-day climate but is more appropriate for the description of climate change. Due to the high sensitivity of F to cloud parameters, the climate projection with this set of parameters could be notably different from that obtained from the standard set of parameters, even though the present-day climate is reproduces adequately.

[24] Note that the aerosol indirect effect can only be realistically estimated using climate models, when the models produce realistic distributions of clouds and cloud water content - in particular for low-level clouds. This is a challenge not only for climate modellers but also for the remote sensing community, as large difficulties remain in accurately observing cloud water content. For future climate, the change in clouds relative to the present-day climate is crucial. Any change in clouds will impact the radiation balance directly - perhaps the dominating effect - and indirectly via the indirect aerosol effect.

[25] **Acknowledgments.** We thank M. Esch and M. Botzet for technical support on ECHAM5. We acknowledge fruitful discussions with B. Stevens, D. Klocke, J. Quaas, U. Lohmann, W. Bauer and the MPI uncertainty working group. We acknowledge partial financial support by the EU-WATCH project (contract 036946).

References

Andreae, M. O., C. D. Jones, and P. M. Cox (2005), Strong present-day aerosol cooling implies a hot future, *Nature*, *435*, 1187.

Boucher, O., and U. Lohmann (1995), The sulfate-CCN-cloud albedo effect: A sensitivity study using two general circulation models, *Tellus, Ser. B*, *47*, 281.

Cahalan, R. F., W. Ridgway, W. J. Wiscombe, and T. L. Bell (1994), The albedo of fractal cumulus clouds, *J. Atmos. Sci.*, *51*, 2434.

Chen, Y., and J. E. Penner (2005), Uncertainty analysis for estimates of the first indirect aerosol effect, *Atmos. Chem. Phys.*, *5*, 2935.

Forster, P., et al. (2007), Changes in atmospheric constituents and in radiative forcing, in *Climate Change 2007: The Physical Science Basis. Contribution of Working Group I to the Fourth Assessment Report of the Intergovernmental Panel on Climate Change*, edited by S. Solomon et al., pp. 129–234, Cambridge Univ. Press, Cambridge, U. K.

Hansen, J., et al. (2005), Efficacy of climate forcings, *J. Geophys. Res.*, *110*, D18104, doi:10.1029/2005JD005776.

Harvey, L. D. D., and R. K. Kaufmann (2002), Simultaneously constraining climate sensitivity and aerosol radiative forcing, *J. Clim.*, *15*, 2837.

Haywood, J., and O. Boucher (2000), Estimates of the direct and indirect radiative forcing due to tropospheric aerosols: A review, *Rev. Geophys.*, *38*, 513.

Kiehl, J. T. (2007), Twentieth century climate model response and climate sensitivity, *Geophys. Res. Lett.*, *34*, L22710, doi:10.1029/2007GL031383.

Knutti, R., and G. C. Hegerl (2008), The equilibrium sensitivity of the Earth's temperature to radiation changes, *Nat. Geosci.*, *1*, 735.

Lohmann, U. (2008), Global anthropogenic aerosol effects on convective clouds in ECHAM5-HAM, *Atmos. Chem. Phys.*, *8*, 2115.

Lohmann, U., J. Feichter, J. Penner, and R. Leaitch (2000), Indirect effect of sulfate and carbonaceous aerosols: A mechanistic treatment, *J. Geophys. Res.*, *105*, 12,193.

McComiskey, A., and G. Feingold (2008), Quantifying error in the radiative forcing of the first aerosol indirect effect, *Geophys. Res. Lett.*, *35*, L02810, doi:10.1029/2007GL032667.

McKay, M. D., R. J. Beckman, and W. J. Conover (1979), A comparison of three methods for selecting values of input variables in the analysis of output from a computer code, *Technometrics*, *21*, 239.

Menon, S., A. D. D. Genio, D. Koch, and G. Tselioudis (2002), GCM simulations of the aerosol indirect effect: Sensitivity to cloud parameterization and aerosol burden, *J. Atmos. Sci.*, *59*, 692.

Murphy, J. M., et al. (2004), Quantifying uncertainty in model predictions, *Nature*, *430*, 768.

Myhre, G., et al. (2004), Uncertainties in the radiative forcing due to sulfate aerosols, *J. Atmos. Sci.*, *61*, 485.

Penner, J. E., et al. (2006), Model intercomparison of indirect aerosol effects, *Atmos. Chem. Phys.*, *6*, 3391.

Piani, C., D. J. Frame, D. A. Stainforth, and M. R. Allen (2005), Constraints on climate change from a multi-thousand member ensemble of simulations, *Geophys. Res. Lett.*, *32*, L23825, doi:10.1029/2005GL024452.

Roeckner, E., L. Bengtsson, J. Feichter, J. Lelieveld, and H. Rodhe (1999), Transient climate change simulations with a coupled atmosphere-ocean GCM including the tropospheric sulfur cycle, *J. Clim.*, *12*, 3004.

Roeckner, E., et al. (2003), The atmospheric general circulation model ECHAM5. Part I: Model description, *Rep. 349*, 127 pp., Max-Planck Inst. für Meteorol., Hamburg, Germany.

Stephens, G. L., S.-C. Tsay, P. W. Stackhouse Jr., and P. J. Flatau (1990), The relevance of the microphysical and radiation properties of cirrus clouds to climate and climatic feedback, *J. Atmos. Sci.*, *47*, 1742.

Tanré, D., J.-F. Geleyn, and J. M. Slingo (1984), First results of the introduction of an advanced aerosol-radiation interaction in the ecmwf low resolution global model, in *Aerosols and Their Climatic Effects*, edited by H. Gerber and A. Deepak, pp. 133–177, A. Deepak, Hampton, Va.

Textor, C., et al. (2006), AeroCom: The status quo of global aerosol modelling, *Atmos. Chem. Phys.*, *6*, 1777.

Tiedtke, M. (1989), A comprehensive mass flux scheme for cumulus parameterization in large-scale models, *Mon. Weather Rev.*, *117*, 1779.

J. O. Haerter, E. Roeckner, L. Tomassini, and J.-S. von Storch, Max Planck Institute for Meteorology, Bundesstr. 53, D-20146 Hamburg, Germany. (jan.haerter@zmaw.de)